THE JOURNAL OF BIOLOGICAL CHEMISTRY
Vol. 278, No. 28, Issue of July 11, pp. 26166–26173, 2003
Printed in U.S.A.

Islet Cell Autoantigen of 69 kDa Is an Arfaptin-related Protein Associated with the Golgi Complex of Insulinoma INS-1 Cells*

Received for publication, December 27, 2002, and in revised form, March 24, 2003
Published, JBC Papers in Press, April 7, 2003, DOI 10.1074/jbc.M213222200

Folker Spitzenberger‡§¶, Susan Pietropaolo‖, Paul Verkade, Bianca Habermann‡‡, Sandra Lacas-Gervais‡, Hassan Mziaut‡, Massimo Pietropaolo‖, and Michele Solimena‡**§§**

*From ‡Experimental Diabetology and the §Department of Internal Medicine III, "Carl Gustav Carus" Medical School, University of Technology Dresden, 01307 Dresden, Germany, the ‖Division of Immunogenetics, Diabetes Institute, University of Pittsburgh School of Medicine, Pittsburgh, Pennsylvania 15213, the **Max Planck Institute for Molecular Cell Biology and Genetics, 01307 Dresden, Germany, and ‡‡Scionics GmbH, 01307 Dresden, Germany*

Islet cell autoantigen of 69 kDa (ICA69) is a cytosolic protein of still unknown function. Involvement of ICA69 in neurosecretion has been suggested by the impairment of acetylcholine release at neuromuscular junctions upon mutation of its homologue gene *ric-19* in *C. elegans*. In this study, we have further investigated the localization of ICA69 in neurons and insulinoma INS-1 cells. ICA69 was enriched in the perinuclear region, whereas it did not co-localize with markers of synaptic vesicles/synaptic-like microvesicles. Confocal microscopy and subcellular fractionation in INS-1 cells showed co-localization of ICA69 with markers of the Golgi complex and, to a minor extent, with immature insulin-containing secretory granules. The association of ICA69 with these organelles was confirmed by immunoelectron microscopy. Virtually no ICA69 immunogold labeling was observed on secretory granules near the plasma membrane, suggesting that ICA69 dissociates from secretory granule membranes during their maturation. *In silico* sequence and structural analyses revealed that the N-terminal region of ICA69 is similar to the region of arfaptins that interacts with ARF1, a small GTPase involved in vesicle budding at the Golgi complex and immature secretory granules. ICA69 is therefore a novel arfaptin-related protein that is likely to play a role in membrane trafficking at the Golgi complex and immature secretory granules in neurosecretory cells.

Originally identified by immunoscreening of an islet cDNA expression library with prediabetic sera, islet cell autoantigen of 69 kDa (ICA69)[1] is an evolutionary conserved gene with homologues in the nonmammalian model organisms *Drosophila melanogaster* and *Caenorhabditis elegans* (1–3). Like most antigens of type 1 diabetes, ICA69 is enriched in pancreatic β-cells and neurons (4). Use of alternative exons in the 5′-untranslated region of the ICA69 gene can affect its tissue expression (5). Although ICA69 deficiency in mice does not induce any obvious phenotype, the knockout of its *C. elegans* homologue compromises neurotransmission (3, 6). This finding has led to the hypothesis that ICA69, despite lacking membrane anchoring signals, is linked to neuronal synaptic vesicles (SVs) and the related synaptic-like microvesicles (SLMVs) of endocrine cells (3).

We now show that ICA69 is mostly associated with the Golgi complex and, to a less extent, with immature secretory granules (ISGs) of insulinoma cells. ICA69 is similar to arfaptins, which act as effectors of the small GTPases ARF and Rac (7, 8). Thus, ICA69 is likely to play a role in vesicular transport regulated by small GTP-binding proteins at the Golgi complex and ISGs in β-cells and secretory cells in general.

EXPERIMENTAL PROCEDURES

Materials—The following antibodies were used: affinity-purified rabbit antibodies against residues 471–483 of human ICA69 (pICA69) (1) and against ICA512 ectodomain (9); mouse monoclonal antibodies against human ICA69 (mICA69); GAD65 (9); β′COP (Drs. J. Fuellekrug and K. Simons, Max Planck Institute for Molecular Cell Biology and Genetics, Dresden, Germany); the 18-kDa fragment of secretogranin II (Dr. S. Tooze, Cancer UK, London, UK) (10, 11); giantin (Dr. H.-P. Hauri, Biozentrum, Basel, Switzerland) (12); TGN38, GM130, syntaxin 6, and carboxypeptidase E/H (BD Transduction Laboratories, Heidelberg, Germany); ARF1 (Affinity Bioreagents, Golden, CO); proinsulin (nonreactive against insulin) (Research Diagnostics); synaptophysin (Synaptic Systems, Goettingen, Germany); transferrin receptor (Zymed Laboratories, South San Francisco, CA); insulin and γ-tubulin (Sigma), goat anti-rabbit and anti-mouse IgGs conjugated to Alexa 488 or Alexa 568 (Molecular Probes, Inc., Eugene, OR); and goat anti-rabbit and goat anti-mouse IgGs conjugated with gold particles (Electron Microscopy Sciences, Fort Washington, PA). All other reagents were from Sigma, unless otherwise specified.

Immunofluorescence—Mouse brains were fixed and immunolabeled as described (13). Rat INS-1 cells, hamster HIT-15, and mouse MIN6 insulinoma cells were cultured and processed as described (13–16). For γ-tubulin staining, cells were fixed with cold methanol (−20 °C) for 5 min and labeled as described (17). Antibodies were diluted as follows: pICA69 (1:200) and mICA69 (1:20). All other antibodies were used according to the providers' instructions. Confocal microscopy was performed with an LSM 510 station (Carl Zeiss, Jena, Germany). For drug treatments, cells were incubated for 1 h or 30 min in normal medium plus 20 μg/ml nocodazole or 2 μg/ml BFA, respectively. For mild destabilization of the microtubule cytoskeleton, cells were processed as described (18).

Biochemical Procedures—Rat brain and INS-1 cells were homogenized and centrifuged as described (19, 20). Postnuclear supernatants (PNS) were spun at 150,000 × *g* for 1 h at 4 °C. The resulting high speed

* This work was supported by grants from the National Institutes of Health (to M. S. and M. P.), the American Diabetes Association (to M. S. and M. P.), and the Alexander von Humboldt Foundation (to M. S.). The costs of publication of this article were defrayed in part by the payment of page charges. This article must therefore be hereby marked "*advertisement*" in accordance with 18 U.S.C. Section 1734 solely to indicate this fact.

¶ Recipient of a Meddrive grant of the Medical School at the University of Technology Dresden.

§§ To whom correspondence should be addressed: Experimental Diabetology, "Carl Gustav Carus" Medical School, University of Technology Dresden, Fetscherstr. 74, 01307 Dresden, Germany. Tel.: 49-351-458-6611; Fax: 49-351-458-6330; E-mail: michele.solimena@mailbox.tu-dresden.de.

[1] The abbreviations used are: ICA69, islet cell autoantigen of 69 kDa; BFA, brefeldin A; CPE, carboxypeptidase E; GAD65, glutamic acid decarboxylase of 65 kDa; ISG, immature secretory granule; MTOC, microtubule organizing center; PNS, postnuclear supernatant; MSGs, mature secretory granules; SG, secretory granule; SVs, synaptic vesicles; SLMVs, synaptic-like microvesicles; TGN, trans-Golgi network.

supernatant was collected while the high speed pellet was brought back to the original volume with homogenization buffer. Protein concentrations were measured with the BCA reagent (Pierce). For Western blotting, proteins were separated by 10% SDS-PAGE and blotted with the following antibodies: pICA69 (1:1,000), mICA69 (1:200), and synaptophysin (1:10,000). Immunoreactivity was detected by chemiluminescence (Amersham Biosciences) using a LAS-1000 Bioimaging System (Fujifilm, Tokyo, Japan). Immunoprecipitation was carried out essentially as described (21). 600 μl of the extracts were incubated overnight at 4 °C with 10 μl of mICA69, 25 μl of pICA69, or 10 μl of rabbit IgGs as a negative control.

In Vitro Transcription/Translation—*In vitro* transcribed/translated [^{35}S]Met-labeled fragments of human ICA69 (N-terminal fragment: residues 1–239; C-terminal fragment: residues 230–483) were incubated with mICA69 for 16 h and then for 45 min with protein G-Sepharose (Amersham Biosciences) at 4 °C. An IgG_1 immunoglobulin was used as negative control. Immunoprecipitates were separated by SDS-PAGE and visualized by exposing autoradiography films for 12–15 h at −80 °C.

[α-^{32}P]GTP Overlay—INS-1 cells were processed for immunoprecipitation as described above. [α-^{32}P]GTP overlay assay was performed as previously described (22). Radiolabeling was detected with the Bio-Imager Analyzer BAS-1800II (Fujifilm).

Subcellular Fractionation—Rat brain subcellular fractions and purified SVs (23) were kindly donated by Dr. W. Huttner (Max Planck Institute for Molecular Cell Biology and Genetics, Dresden, Germany) and Dr. R. Jahn (Max Planck Institute for Biophysical Chemistry, Goettingen, Germany). Fractions were immunoblotted with pICA69 and synaptophysin antibodies. Fractionation of INS-1 cells on continuous sucrose density gradients (0.4–1.8 M sucrose) was performed as described (24–26). Fractions were immunoblotted for ICA69 (pICA69), synaptophysin, TGN38 (1:200), GM130 (1:200), syntaxin 6 (1:500), transferrin receptor (1:2,500), carboxypeptidase E (CPE) (1:2,000), and the 18-kDa fragment of secretogranin II (1:400). Semiquantitative measurement was performed with the Image Reader 2.2 software of the LAS-1000 imaging system (Fujifilm).

Immunoelectron Microscopy—Immunoelectron Microscopy on gradient fractions was performed as described (27) using antibodies pICA69 (1:50) and anti-TGN38 (1:25) followed by goat anti-rabbit and anti-mouse antibodies conjugated with 10- and 6-nm gold particles, respectively. Immunoelectron microscopy on ultrathin cryostat sections was performed as described (28) with minor variations. INS-1 cells were fixed with 4% paraformaldehyde and 0.05% glutaraldehyde in phosphate-buffered saline. Sections were simultaneously labeled with pICA69 (1:10) and anti-giantin (1:10) or anti-insulin (1:100) antibodies, followed by 6- and 12-nm gold-conjugated anti-mouse and anti-rabbit antibodies, respectively. As controls, primary antibodies were omitted.

Data Base Searches and Structural Predictions—Data base searches were carried out with the programs BLASTP and PSI-BLAST (29) using standard parameters against the nonredundant NCBI protein data base (release of November 27, 2001). Multiple sequence alignments were produced with the program ClustalX (30, 31) and manually re-

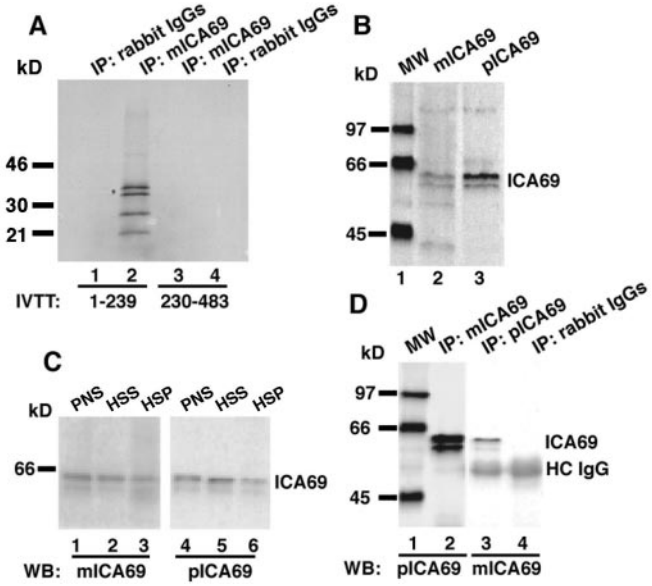

FIG. 1. **Recognition of ICA69 by two antibodies against distinct ICA69 epitopes.** *A*, [^{35}S]Met-labeled *in vitro* transcribed/translated (*IVTT*) N-terminal (amino acids 1–239; *lanes 1* and *2*) and C-terminal (amino acids 230–483; *lanes 3* and *4*) fragments of human ICA69 immunoprecipitated (*IP*) with mICA69 (*lanes 2* and *4*) or nonspecific IgG1 as control (*lanes 1* and *3*). Analysis of immunoprecipitates by SDS-PAGE and autoradiography showed that mICA69 recognizes an epitope located within the N-terminal half of ICA69. *B* and *C*, Western blotting with mICA69 (*B*, *lane 2*; *C*, *lanes 1–3*) and pICA69 (*B*, *lane 3*; *C*, *lanes 4–6*) on rat brain PNS (*B*) and INS-1 cell fractions (*C*). ICA69 (60-kDa doublet) is present in the PNS, high speed supernatant (*HSS*), and high speed pellet (*HSP*) of INS-1 cells. *D*, following cross-immunoprecipitation and Western blotting (*WB*), pICA69 (*lane 2*) and mICA69 (*lane 3*) recognized the same 60-kDa protein doublet. Nonspecific rabbit IgGs were used for immunoprecipitation as controls (*lane 4*).

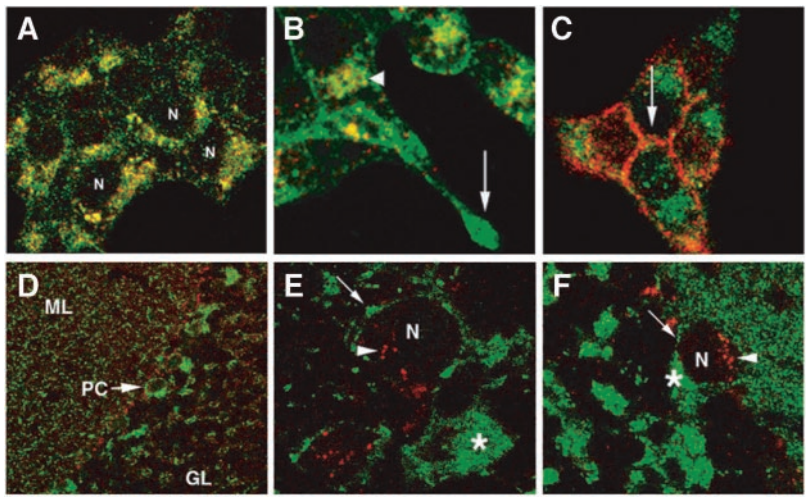

FIG. 2. **Confocal microscopy for ICA69 and markers of SLMVs, SVs, and SGs.** *A*, mICA69 (*pseudogreen*) and pICA69 (*pseudored*) produced a nearly identical staining pattern in the perinuclear region of INS-1 cells (*orange-yellow pseudocolor*). *N*, nucleus. *B*, high power magnification of INS-1 cells double stained for ICA69 (*pseudored*) and synaptophysin (*pseudogreen*). While synaptophysin was enriched at neurite-like cell extensions (*long arrow*), ICA69 was concentrated in the perinuclear region (*arrowhead*). *C*, ICA69 (*pseudogreen*) did not co-localize with ICA512 (*pseudored*), a protein enriched in MSGs. *D–F*, distribution of ICA69 (*pseudored*) in mouse brain. Double labelings with GAD65 (*D* and *E*) and synaptophysin (*F*) as markers of SVs (both in *pseudogreen*). *D*, ICA69 immunoreactivity was prominent in Purkinje cells (*PC*, *arrow*), but not in the molecular layer (*ML*) or granular layer (*GL*), where most synaptic terminals of the cerebellar cortex are found. *E* and *F*, high power magnifications showing that ICA69 is associated with perinuclear structures (*arrowheads*), whereas it does not co-localize with GAD65 (*E*) or synaptophysin (*F*) in synaptic terminals around the cell bodies (*arrows*) and axon hillocks (*asterisks*) of Purkinje cells.

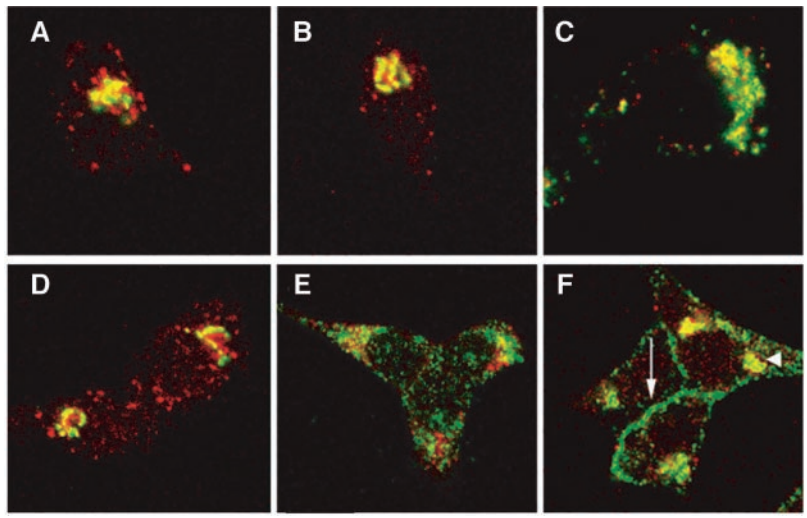

FIG. 3. **Confocal microscopy for ICA69 (*pseudored*), markers of the Golgi complex and SGs in rat insulinoma INS-1 cells (*pseudogreen*).** ICA69 overlaps significantly with TGN38 (*A*) and giantin (*B*). Partial overlap was also found with β'COP (*C*), with which the co-localization extended to structures outside the Golgi region, and with GM130 (*D*). Double labelings for ICA69 and proinsulin showed some co-distribution in the perinuclear region (*E*). *F*, ICA69 co-distributed with insulin in the perinuclear area (*arrowhead*) but not near the plasma membrane, where MSGs accumulate (*long arrow*).

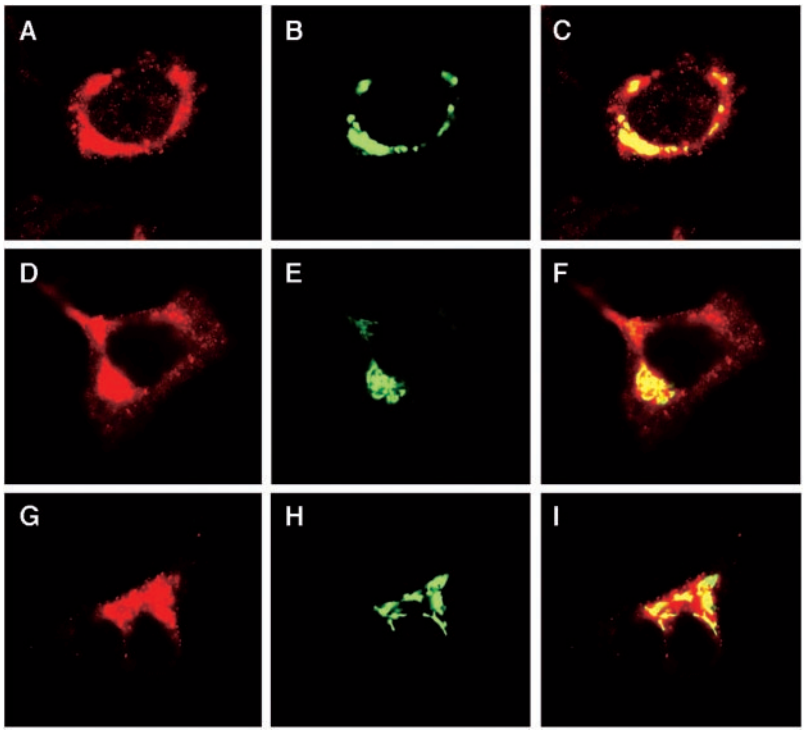

FIG. 4. **Confocal microscopy for ICA69 (*pseudored*, *left panels*) and markers of the Golgi complex (*pseudogreen*, *central panels*) in hamster HIT (*A–F*) and mouse MIN6 (*G–I*) insulinoma cells.** ICA69 partially overlaps significantly with TGN38 (*A–C*) and GM-130 (*D–I*). *Merged images* are shown in the *right panels*.

fined. Structure prediction was done using the programs 3D-PSSM (32) and PredictProtein (33).

RESULTS

Characterization of Two Antibodies Directed against Distinct Epitopes of ICA69—The localization of ICA69 in neurons and insulinoma cells was investigated by employing two distinct antibodies directed against ICA69. The first antibody consists of affinity-purified rabbit IgGs (polyclonal ICA69, or pICA69), which were raised against residues 471–483 at the C-terminal end of ICA69 (1). The second antibody was a monoclonal IgG (mICA69), which was obtained by mouse immunization with full-length recombinant ICA69 expressed in bacteria as a fusion protein with glutathione *S*-transferase. To map the epitope recognized by mICA69, the N-terminal (amino acids 1–239) and C-terminal (amino acids 230–483) halves of ICA69 were independently expressed as ^{35}S-labeled polypeptides by *in vitro* transcription/translation and incubated either with mICA69 or control mouse IgG for immunoprecipitation followed by SDS-PAGE and autoradiography (Fig. 1*A*). This analysis shows that mICA69 selectively immunoprecipitated the N-terminal ICA69 polypeptide, whereas control mouse IgG did not react with either ICA69 fragment. Whereas the N-terminal fragment of ICA69 has a molecular mass of 28 kDa, it migrated as a 35-kDa protein by SDS-PAGE. The aberrant electrophoretic mobility of the N-terminal domain may account for the overall slower migration of native ICA69, which has a molecular mass of 54.6 kDa but migrates as a 60-kDa protein under the present conditions for SDS-PAGE (1) (Fig. 1*B*). By Western blotting on PNS from rat brain (Fig. 1*B*) and INS-1 cells (Fig. 1*C*), both mICA69 and pICA69 antibodies recognized indeed a protein doublet of 60 kDa (R_f = 0.34 and 0.37, respectively). Given its detection with two antibodies directed against distinct ICA69 epitopes, this 60-kDa protein doublet is likely to represent ICA69. The amino acid sequence of ICA69 contains a second methionine at position 26. Initiation of translation at this alternative methionine may explain the presence of a protein doublet upon *in vitro* translation (Fig. 1*A*) and in cell extracts (Fig. 1, *B* and *C*). Moreover, mICA69 and pICA69

antibodies immunoprecipitated the same 60-kDa protein doublet from INS-1 cell extracts (Fig. 1*D*) and produced an identical particulate staining by immunocytochemistry (Fig. 2*A*). Partitioning of ICA69 between cytosolic and particulate fractions (Fig. 1*C*) suggested that a pool of the protein is membrane-associated, despite lacking membrane targeting motifs.

ICA69 Is Not Enriched in Neuronal Synaptic Vesicles and Synaptic-like-Microvesicles of INS-1 Cells—Previous studies suggested an association of ICA69 with neuronal SVs and SLMVs of insulinoma cells (3). Double immunofluorescence on INS-1 cells, however, showed that ICA69 immunoreactivity was concentrated in the perinuclear region (Fig. 2*A*), whereas virtually no signal was found at the tip of neurite-like extensions where synaptophysin and SLMVs are concentrated (Fig. 2*B*) (34, 35). ICA69 distribution was also different from that of ICA512, a protein enriched in mature secretory granules (MSGs) near the plasma membrane (Fig. 2*C*) (9). Double immunofluorescence on mouse cerebellar sections showed that ICA69 is found in the perinuclear region of Purkinje cells (Fig. 2, *D–F*). This pattern did not resemble that of GAD65, which is associated with SVs of GABA-ergic synapses around Purkinje cells and throughout the cerebellar cortex (Fig. 2, *D* and *E*) (24, 36). There was also no co-localization of ICA69 with synaptophysin (Fig. 2*F*), a general marker of SVs and synaptic terminals (34). Similar observations were made upon subcellular fractionation of rat brain synaptosomes. As expected (37), synaptophysin was concentrated in the LP2 fraction (crude SVs) and further enriched in the sucrose-gradient vesicle fraction (purified SVs), whereas ICA69 was most abundant in the LP1 (large membranes and cytoskeleton) and LS2 (synaptosol) fractions (not shown). These data indicated that ICA69 is neither enriched on neuronal SVs nor on SLMVs and MSGs of insulinoma cells.

Localization of ICA69 to the Golgi Complex and Immature Secretory Granules by Confocal Microscopy—We compared the perinuclear pattern of ICA69 with that of proteins enriched in the Golgi compartment of INS-1 cells (Fig. 3, *A–F*). ICA69 was co-localized in part with TGN38 (Fig. 3*A*) and giantin (Fig. 3*B*). Giantin is a general marker of the Golgi complex (12), whereas TGN38 is enriched at the trans-Golgi network (TGN) (38, 39). ICA69 also partially overlapped with the peripherally associated Golgi proteins β′COP (Fig. 3*C*) (40–43) and GM130 (Fig. 3*D*) (44). Finally, ICA69 overlapped in part with proinsulin, which is found in ISGs, but not in MSGs (Fig. 3*E*) (45, 46). It also co-distributed with insulin in the Golgi region but not near the plasma membrane (Fig. 3*F*). The significant, albeit partial, colocalization of ICA69 with Golgi markers GM-130 and TGN38 was confirmed in hamster insulinoma HIT-cells and mouse insulinoma MIN-6 cells (Fig. 4, *A–I*). These results suggested that ICA69 is broadly associated with the Golgi complex and, to a much lesser extent, with ISGs.

Localization of ICA69 at the Golgi Complex and Immature Secretory Granules by Immunoelectron Microscopy—By immunoelectron microscopy on cryoultrathin sections of INS-1 cells, ICA69 was found on Golgi stacks close to giantin (Fig. 5*A*) and at budding sites of vesicles from the Golgi complex (Fig. 5*B*) and SGs (Fig. 5*C*). Overall, ICA69 was found on a minority of SGs (Fig. 5*E*), as identified by double gold immunolabeling with insulin (not shown). ICA69-positive SGs were most abundant in the central region of the cell (Fig. 5*D*), with a mean distance from the plasma membrane that was about twice the mean distance of ICA69-negative SGs and SGs in general (Fig. 5*F*). These data indicated that ICA69 is associated with the Golgi complex, whereas a minor pool is also found on ISGs, which are significantly more distant from the plasma membrane than the total of the SGs.

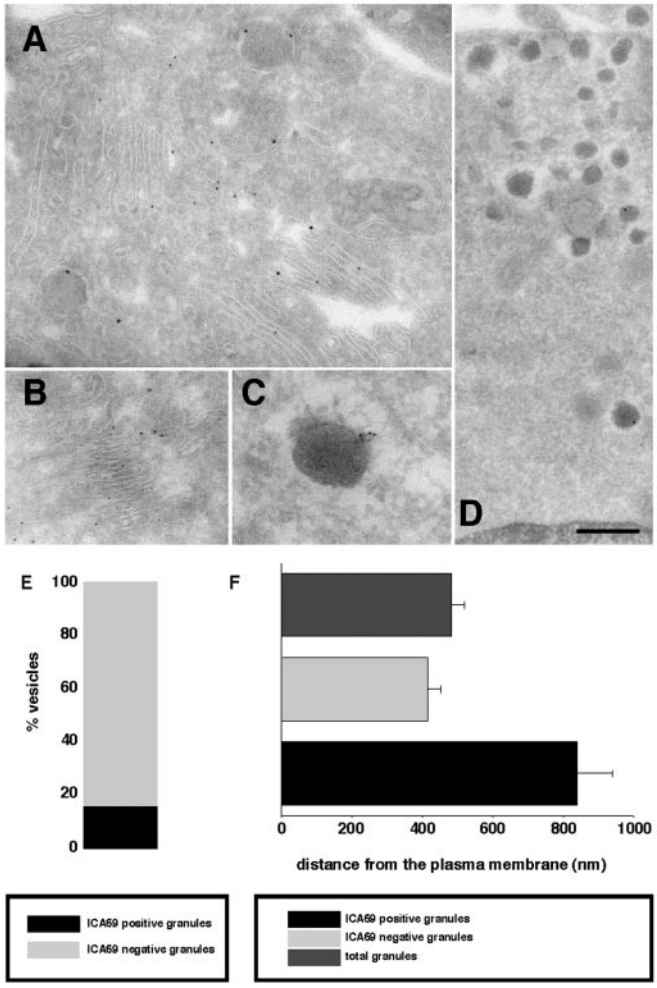

FIG. 5. **Ultrastructural localization of ICA69 in INS-1 cells.** In double labelings, the staining with the pICA69 antibody (12-nm gold) was compared with the staining for giantin (6-nm gold). ICA69 co-localizes with giantin on Golgi cisternae (*A*). In addition, it is found on SGs (*A*), which sometimes seem to be budding from the Golgi (*B*). *C*, ICA69 is also present on vesicles which appear to emerge from SGs. *D*, ICA69-negative SGs concentrate near the plasma membrane of INS-1 cells, whereas ICA69-positive SGs are preferentially found toward the cell center. *E*, ICA69 was detected on 27 (15.7%) of 172 SGs counted in 10 INS-1 cells. *F*, the mean distance of the ICA69-positive SGs from the plasma membrane (840 nm, S.E. = 99 nm) was about twice the mean distance of the ICA69-negative SGs (415 nm, S.E. = 37 nm; $p = 0.000022$) and of the overall mean distance of all measured SGs from the plasma membrane (482 nm, S.E. = 37 nm, $p = 0.00057$). The *bar* in *D* represents 150 nm for *A* and *B*, 100 nm for *C*, and 250 nm for *D*.

Enrichment of ICA69 on the Golgi Complex by Subcellular Fractionation—Fractionation of INS-1 cell extracts on sucrose density gradients separated two main peaks of ICA69 at 0.9 and 1.1 M sucrose (Fig. 6*A*). These fractions included the peaks of the TGN proteins TGN38 and syntaxin 6 (0.9 M sucrose) and the early Golgi marker GM130 (1.1 M sucrose) (Fig. 6*B*, *left panel*). The soluble pools of ICA69 and GM130 were recovered in light fractions (0.4–0.5 M sucrose), whereas low levels of ICA69 were detected in 1.2–1.4 M sucrose fractions. These last fractions contained the first peak of the SG marker CPE (Fig. 6*B*, *middle panel*), indicating the presence of ISGs, which are lower in density than the MSGs. A second pool of CPE was found in denser fractions (1.5–1.7 M sucrose) together with p18, a marker of MSGs (11, 47). The peaks of ICA69 were slightly shifted from those of synaptophysin and transferrin receptor, which overlapped in 1.0 M sucrose fractions (Fig. 6*B*, *right panel*) (48). The gradient fractions were also examined by immunoelectron microscopy. The 0.9 M sucrose fraction contained

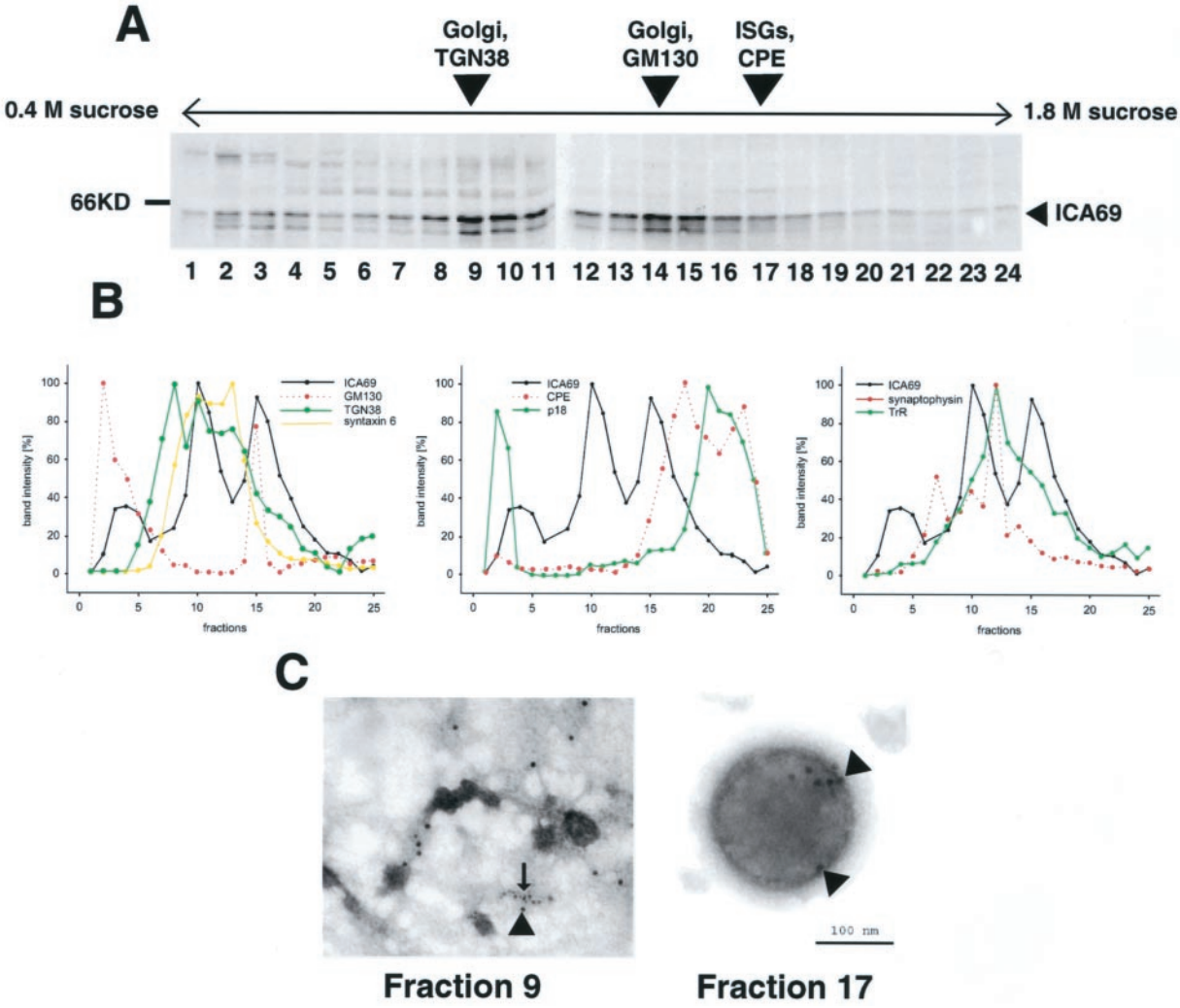

FIG. 6. **Distribution of ICA69 by subcellular fractionation of INS-1 cells on sucrose density gradients (0.4–1.8 M).** *A*, equal volumes of each fraction were immunoblotted with pICA69. *B*, profile distribution of different organelle markers in the gradients as determined by immunoblotting and chemiluminescence. Levels of ICA69 were compared with those of TGN38, syntaxin 6, and GM130 as Golgi markers (*B*, *left panel*), CPE and p18 as SG markers (*B*, *middle panel*), and synaptophysin and transferrin receptor as markers of SLMVs and recycling endosomes, respectively (*B*, *right panel*). ICA69 mostly co-distributed with late and early Golgi markers (fractions 9 and 14, 0.9 and 1.1 M sucrose, respectively) and to a lesser extent with the first peak of CPE (fractions 16–18, 1.2–1.4 M sucrose), corresponding to ISGs. *C*, fractions 9 (0.9 M sucrose) and 17 (1.35 M sucrose) were examined by immunoelectron microscopy. Fraction 9 (*left panel*) contained Golgi-like structures positive for ICA69 (12-nm gold, *arrowhead*) and TGN38 (6-nm gold, *arrow*); fraction 17 (*right panel*) was enriched in SGs positive for ICA69. Sucrose molarity was as follows: 0.43 ± 0.02 M (fraction 1); 0.74 ± 0.02 M (fraction 5), 0.93 ± 0.03 M (fraction 10), 1.16 ± 0.04 M (fraction 15), 1.46 ± 0.07 M (fraction 20), 1.84 ± 0.04 M (fraction 25).

membranous, ribbon-like structures that resemble Golgi stacks and were positive for ICA69 and TGN38 (Fig. 6*C*, *left panel*), whereas the 1.35 M sucrose fraction contained SGs positive for ICA69 (Fig. 6*C*, *right panel*). These data confirmed the association of ICA69 with Golgi membranes and, to a lesser extent, with ISGs.

The Distribution of ICA69 Is Nocodazole- and BFA-sensitive—We analyzed whether drugs that affect the organization of the Golgi complex alter the distribution of ICA69 in INS-1 cells. Nocodazole treatment caused a major loss of ICA69 immunoreactivity in the perinuclear region (Fig. 7*A*). Some ICA69, however, could still be detected on TGN38-labeled Golgi fragments scattered throughout the cells. Treatment of cells with nocodazole followed by taxol causes a redistribution and mild destabilization of the microtubule cytoskeleton similar to what occurs in the prophase of mitosis (18, 49). In these conditions, ICA69 had a bipolar distribution that overlapped with TGN38 at opposite sides of the nucleus (Fig. 7*B*), near the centrioles (Fig. 7*C*). BFA causes the release of coatomers from Golgi membranes and the retrieval of resident Golgi enzymes into the endoplasmic reticulum by inhibiting guanine nucleotide exchange on ARF (50). It also leads to the formation of a hybrid TGN-endosomal system near the microtubule-organizing center (MTOC) by inhibiting the TGN-endosome recycling pathway (51–54). ICA69 immunoreactivity was significantly reduced upon BFA treatment (compare Fig. 7, *D–F*, with Figs. 2, 3, and 7, *B* and *C*), suggesting a redistribution of ICA69 in the cytosol, similar to what has been shown for β′COP (55). A pool of ICA69, however, retained a juxtanuclear position within one or two brightly stained clusters that were distinct from GM130-positive Golgi remnants (Fig. 7*E*) (44, 56) but that still contained some TGN38 (Fig. 7*D*) and especially syntaxin 6 (Fig. 7*F*). Syntaxin 6 participates in the TGN-endosomal recycling pathway and is also found on ISGs (11, 57). These observations implied that the perinuclear concentration of ICA69 is microtubule-dependent and emphasized the relationship of ICA69 with the Golgi complex.

ICA69 Is Related to Arfaptin—Iterated BLAST searches with the ICA69 sequence against current protein data bases indicated that the N-terminal region of ICA69 is significantly sim-

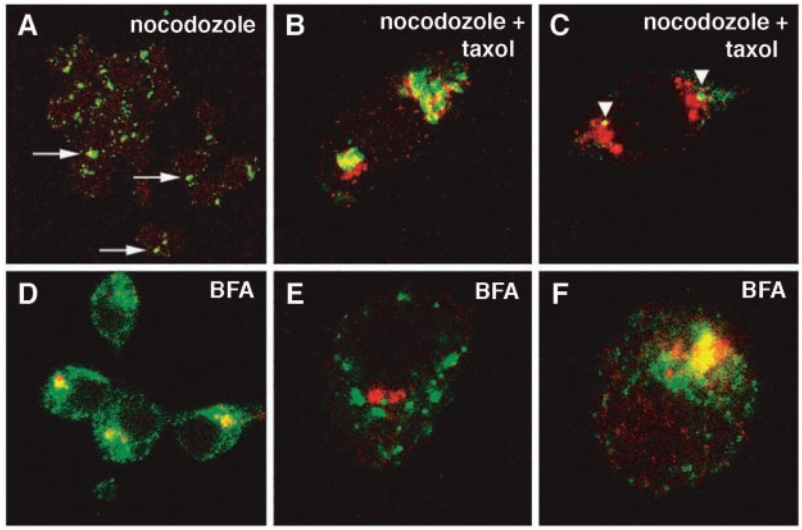

FIG. 7. **ICA69 distribution upon pharmacological treatments of INS-1 cells.** *A*, after nocodazole treatment, the perinuclear staining for ICA69 (*pseudored*) disappeared. Residual ICA69 labeling was associated with TGN38-positive Golgi fragments (*pseudogreen*) (*A*, *arrows*). *B*, upon mild destabilization of the microtubule cytoskeleton by nocodazole/taxol treatment, ICA69 immunoreactivity (*pseudored*) overlapped with TGN38 (*pseudogreen*) in a bipolar manner at opposite sides of the nucleus, near the centrioles, as visualized with anti-γ-tubulin antibody (*pseudogreen*) (*C*). *D*, BFA treatment reduced ICA69 immunoreactivity, whereas the integral membrane protein TGN38 redistributed to the endoplasmic reticulum. *E*, the residual ICA69 immunoreactivity was concentrated in one or two bright clusters close to the MTOC (*not shown*), which did not overlap with GM130-positive structures (*pseudogreen*) (*E*). A large fraction of ICA69 co-localized instead with syntaxin 6 (*pseudogreen*) (*F*).

ilar to arfaptins (Fig. 8*A*), with an expect value of 2*e*-70 at convergence of PSI-BLAST searching. Back PSI-BLAST searches with human arfaptin 1 identified the ICA69 family with an expect value of 9*e*-73 at the third iteration. Arfaptin 1 and 2 are cytosolic proteins that bind small GTPases of the ARF family (8) and Rac1 (7). Arfaptin 1, in particular, is recruited to Golgi membranes by ARF1-GTP and acts as negative regulator of ARF1 function (8, 58, 59). Arfaptin is composed of three α-helices that dimerize to form the binding interface for small GTPases. Both dimer subunits contribute to a domain that is structurally related to the Dbl homology domain of Tiam, a guanine nucleotide exchange factor for Rac (60–62). The secondary structure of ICA69 N-terminal half is predicted to be primarily α-helical (Fig. 8*A*) and coincides with that of human arfaptin 2, as deduced from its tertiary structure (63). Thus, it is likely that ICA69 folds like arfaptins and that ICA69 dimerization generates a Dbl homology-like domain that binds small GTPases. Through this interaction, ICA69 may participate in regulating membrane trafficking at the Golgi complex and ISGs. These functional implications were sustained by the finding that both mICA69 and pICA69 antibodies co-immunoprecipitated a yet unidentified small GTP-binding protein from INS-1 cell extracts (Fig. 8*B*). This small GTP-binding protein comigrated with ARF1 (Fig. 7*B*) but did not react with the anti-ARF1 antibody following immunoblotting of the material immunoprecipitated by the ICA69 antibodies (not shown). Interestingly, several of the residues involved in the binding of arfaptin 2 to small GTPases are not conserved in ICA69 (Fig. 8*A*), suggesting that ICA69 may interact with small GTPases other than ARF1 or Rac1.

DISCUSSION

We have shown here that ICA69 is peripherally associated with the Golgi complex and ISGs. This conclusion is consistent with results obtained by confocal microscopy, immunoelectron microscopy, and subcellular fractionation. Additional support for these findings has been obtained using pharmacological treatments that affect the organization of the Golgi complex and post-Golgi membrane compartments.

Previous studies suggested that the *C. elegans* homologue of ICA69, termed *ric-19*, is associated with neuronal SVs (3). A deletion mutant of *ric-19*, in particular, was shown to confer resistance to the acetylcholinesterase inhibitor aldicarb, thus implying a reduced secretion of acetylcholine from SVs at neuromuscular junctions. Confocal microscopy on brain sections, however, did not reveal a co-localization of ICA69 with SV markers. In INS-1 cells ICA69 also did not co-distribute with markers of SLMVs, the counterpart of neuronal SVs in peptide-secreting endocrine cells (64). Furthermore, ICA69 was not found on purified brain SVs nor co-distributed with SLMVs upon fractionation of INS-1 cells. Thus, our data do not support the notion that ICA69 is enriched on SVs/SLMVs. This conclusion, however, is not in conflict with the observation that mutation of *ric-19* hinders the secretion of acetylcholine. Impaired secretion may result from alterations in membrane trafficking upstream of SVs/SLMVs.

Our findings point to a tight connection of ICA69 with the trans-face of the Golgi complex, from which SGs and precursors of SVs/SLMVs originate. Immunoelectron microscopy showed the presence of ICA69 on SGs in the process of budding from the TGN. Upon microtubule disruption (nocodazole treatment), microtubule reorganization (nocodazole, taxol treatment), Golgi-endoplasmic reticulum fusion and TGN-endosome fusion (BFA treatment), a pool of ICA69 remained associated with membranes positive for TGN38. Upon treatment with BFA, ICA69 also co-localized extensively with syntaxin 6 near the MTOC. Syntaxin 6 is a soluble *N*-ethylmaleimide-sensitive attachment protein receptor protein of the TGN and early endosomes (65) that was shown to redistribute around the MTOC in BFA-treated cells (66).

Besides being enriched at the TGN, a minor pool of ICA69 is found on ISGs, whereas it is virtually absent from MSGs. Occasionally, ICA69 was detected on what appeared to be small vesicles pinching off the membrane of SGs. Whereas the presence of a coat was not readily apparent, such profiles could conceivably represent budding clathrin-coated vesicles that remove proteins not destined to MSGs (57, 67, 68). Protein removal from ISGs is part of the maturation process that leads to the formation of MSGs (69, 70). The departure of ICA69 from ISGs together with these vesicles could explain its absence on MSGs. In this respect, ICA69 resembles again syntaxin 6,

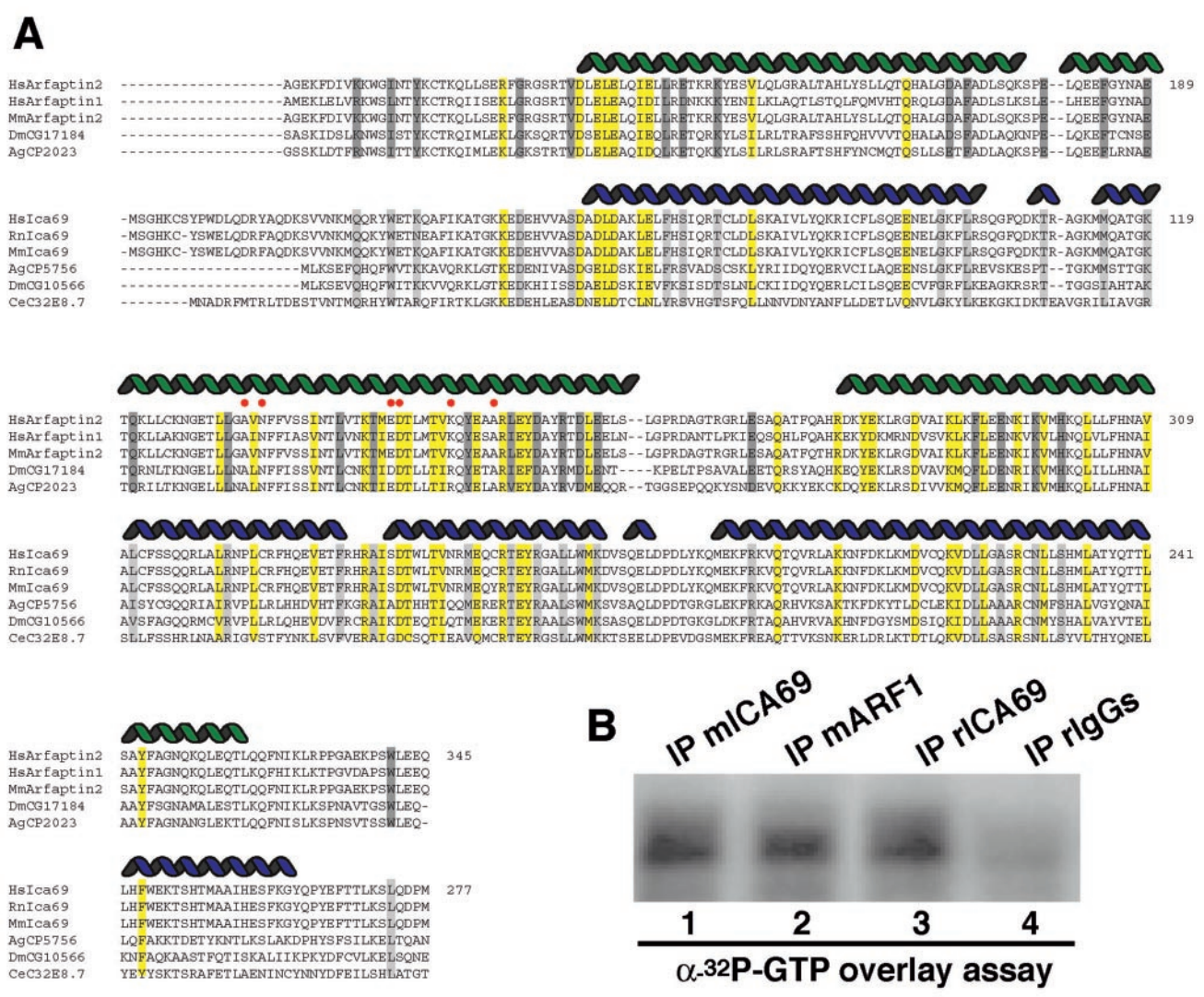

FIG. 8. **ICA69 is related to arfaptins.** *A*, sequence alignment of the N-terminal region of human ICA69 (residues 1–274) and ICA69 homologues with members of the arfaptin family from different species (*Hs*, *Homo sapiens* (arfaptin 1, NP_055262; arfaptin 2, NP_036534; Ica69, NP_071682); *Mm*, *Mus musculus* (arfaptin 2, BAB26070; Ica69, XP_193008); *Rn*, *Rattus norvegicus* (Ica69, NP_110471); *Dm*, *Drosophila melanogaster* (arfaptin, NP_650058; Ica69, NP_649283); *Ag*, *Anopheles gambiae* (arfaptin, EAA10493; Ica69, EAA11288); *Ce*, *Caenorhabditis elegans* (Ica69, NP_491216)). Conserved residues are highlighted in *yellow*. Residues highlighted in *dark gray* (arfaptin family) or *light gray* (ICA69 family) are conserved within the arfaptin or ICA69 family but differ between the two. The *red circles* indicate conserved residues among arfaptins that participate in the binding between arfaptin 2 and Rac1 (63) but that significantly differ in ICA69. α-Helices of arfaptin and ICA69 are shown in *green* and *blue*, respectively. *B*, [α-^{32}P]GTP overlay assay on immunoprecipitates (*IP*) from INS-1 cell extracts obtained with mICA69 (*lane 1*), pICA69 (*lane 3*), and mouse anti-ARF1 (*lane 2*) or rabbit pre-immune IgGs (*lane 4*) as positive and negative controls, respectively. Both anti-ICA69 antibodies immunoprecipitated an unidentified small GTP-binding protein.

which is also associated with ISGs but not with MSG of β-cells (11, 57). Additional studies will be necessary to determine whether ICA69 plays an active role in the maturation process of ISGs.

The similarity of ICA69 with arfaptins strongly suggests that ICA69 participates in membrane trafficking. Arfaptin 1 binds to ARF proteins in their GTP-bound conformation (8). ARFs, in turn, regulate membrane dynamics by promoting the recruitment of coat proteins on membranes as well as by affecting the activity of phospholipid-modifying enzymes and the organization of the actin cytoskeleton (71, 73). In addition to ARFs, arfaptin 2 can also bind Rac and has therefore been proposed as a potential mediator of cross-talk between ARF and Rac (7, 63, 74). Given the sequence similarity of the N-terminal region of ICA69 with the arfaptin Dbl homology-like domain, it is conceivable that ICA69 dimers might also bind small GTPases. Additional studies will be required to identify its binding partners. Thus, our findings raise the possibility that ICA69 acts in concert with small GTPases in regulating membrane dynamics at the Golgi complex and ISGs. The wide tissue expression of ICA69 (1, 4, 5), suggests that this regulation may not be restricted to neuroendocrine cells.

Evidence that ICA69 is found on the TGN and ISGs of INS-1 cells provides additional support to the notion that in type 1 diabetes autoantibodies are preferentially directed toward proteins associated with the post-Golgi secretory machinery of β-cells (75). Interestingly, ICA69 has also been recently identified as an autoantigen in Sjögren's syndrome (6), an autoimmune disorder that affects primarily the exocrine cells of the salivary gland. Autoantibodies of patients with Sjogren's syndrome are typically directed against proteins associated with the Golgi complex (76). The association of ICA69 with Golgi membranes and insulin-containing secretory granules could therefore account for the occurrence of ICA69 autoimmunity in both Sjogren's syndrome and type 1 diabetes. Future studies will determine the contribution of ICA69 to membrane traffick-

ing and the significance of autoimmunity against ICA69 in diseases affecting secretory cells.

Acknowledgments—We thank P. De Camilli for critical discussion and reading of the manuscript; A. De Matteis for discussion and sharing preliminary data on the relationship of ICA69 with arfaptins; W. Huttner and R. Jahn for purified SV preparations; M. Wilsch-Bräuniger for advice; J. Fuellekrug, K. Simons, S. Tooze, G. Warren, H.-P. Hauri, and J. Saraste for the gift of antibodies; and P. Meda and R. Sherwin for insulinoma cell lines. We thank J. Graessler and H.-E. Schroeder for encouragement, I. Unfried for skillful technical support, and K. Pfriem for excellent assistance.

REFERENCES

1. Pietropaolo, M., Castano, L., Babu, S., Buelow, R., Kuo, Y. L. S., Martin, S., Martin, A., Powers, A. C., Prochazka, M., Naggert, J., Leiter, E. H., and Eisenbarth, G. S. (1993) *J. Clin. Invest.* **92,** 359–371
2. Adams, M. D., Celniker, S. E., Holt, R. A., Evans, C. A., Gocayne, J. D., Amanatides, P. G., Scherer, S. E., Li, P. W., Hoskins, R. A., Galle, R. F., George, R. A., Lewis, S. E., Richards, S., Ashburner, M., Henderson, S. N., *et al.* (2000) *Science* **287,** 2185–2195
3. Pilon, M., Peng, X.-R., Spence, A. M., Plasterk, R. H. A., and Dosch, H. M. (2000) *Mol. Biol. Cell* **11,** 3277–3288
4. Karges, W., Pietropaolo, M., Ackerley, C. A., and Dosch, H. M. (1996) *Diabetes* **45,** 513–521
5. Friday, R. P., Pietropaolo, S. L., Profozich, J., Trucco, M., and Pietropaolo, M. (2003) *J. Biol. Chem.* **278,** 853–863
6. Winer, S., Aststurov, I., Gaedigk, R., Hammond-McKibben, D., Pilon, M., Song, A., Kubiak, V., Karges, W., Arpaia, E., McKerlie, C., Zucker, P., Singh, B., and Dosch, H.-M. (2002) *J. Immunol.* **168,** 475–482
7. Van Aelst, L., Joneson, T., and Bar-Sagi, D. (1996) *EMBO J.* **15,** 3778–3786
8. Kanoh, H., Williger, B.-T., and Exton, J. H. (1997) *J. Biol. Chem.* **272,** 5421–5429
9. Solimena, M., Dirkx, R. J., Hermel, J. M., Pleasic-Williams, S., Shapiro, J. A., Caron, L., and Rabin, D. U. (1996) *EMBO J.* **15,** 2102–2114
10. Dittie, A. S., and Tooze, S. A. (1995) *Biochem. J.* **310,** 777–787
11. Wendler, F., Page, L., Urbé, S., and Tooze, S. A. (2001) *Mol. Biol. Cell* **12,** 1699–1709
12. Linstedt, A. D., and Hauri, H. P. (1993) *Mol. Biol. Cell* **4,** 679–693
13. De Camilli, P., Harris, S. M. J., Huttner, W. B., and Greengard, P. (1983) *J. Cell Biol.* **96,** 1355–1373
14. Santerre, R. F., Cook, R. A., Crisel, R. M., Sharp, J. D., Schmidt, R. J., Williams, D. C., and Wilson, C. P. (1981) *Proc. Natl. Acad. Sci. U. S. A.* **78,** 4339–4343
15. Miyazaki, J., Araki, K., Yamato, E., Ikegami, H., Asano, T., Shibasaki, Y., Oka, Y., and Yamamura, K. (1990) *Endocrinology* **127,** 126–132
16. Asfari, M., Janjic, D., Meda, P., Li, G., Halban, P. A., and Wollheim, C. B. (1992) *Endocrinology* **130,** 167–178
17. Zheng, Y., Jung, M. K., and Oakley, B. R. (1991) *Cell* **65,** 817–823
18. Walenta, J. H., Didier, A. J., Liu, X., and Kramer, H. (2001) *J. Cell Biol.* **152,** 923–934
19. Berghs, S., Aggujaro, D., Dirkx, R., Jr., Maksimova, E., Stabach, P., Hermel, J. M., Zhang, J. P., Philbrick, W., Slepnev, V., Ort, T., and Solimena, M. (2000) *J. Cell Biol.* **151,** 985–1002
20. Solimena, M., Dirkx, R. J., Radzynski, M., Mundigl, O., and De Camilli, P. (1994) *J. Cell Biol.* **126,** 331–341
21. Ort, T., Maksimova, E., Dirkx, R., Kachinsky, A. M., Berghs, S., Froehner, S. C., and Solimena, M. (2000) *Eur. J. Cell Biol.* **79,** 621–630
22. Huber, L. A., Pimplikar, S., Parton, R. G., Virta, H., Zerial, M., and Simons, K. (1993) *J. Cell Biol.* **123,** 35–45
23. Huttner, W. B., Schiebler, W., Greengard, P., and De Camilli, P. (1983) *J. Cell Biol.* **96,** 1374–1388
24. Reetz, A., Solimena, M., Matteoli, M., Folli, F., Takei, K., and De Camilli, P. (1991) *EMBO J.* **10,** 1275–1284
25. Iezzi, M., Escher, G., Meda, P., Charollais, A., Baldini, G., Darchen, F., Wollheim, C. B., and Regazzi, R. (1999) *Mol. Endocrinol.* **13,** 202–212
26. Ort, T., Voronov, S., Guo, J., Zawalich, K., Froehner, S. C., Zawalich, W., and Solimena, M. (2001) *EMBO J.* **20,** 4013–4023
27. Krichevsky, A. M., and Kosik, K. S. (2001) *Neuron* **32,** 683–696
28. Scheiffele, P., Verkade, P., Fra, A. M., Virta, H., Simons, K., and Ikonen, E. (1998) *J. Cell Biol.* **140,** 795–806
29. Altschul, S. F., Madden, T. L., Schäffer, A. A., Zhang, J., Zhang, Z., Miller, W., and Lipman, D. J. (1997) *Nucleic Acids Res.* **25,** 3389–3402
30. Thompson, J. D., Gibson, T. J., Plewniak, F., Jeanmougin, F., and Higgins, D. G. (1997) *Nucleic Acids Res.* **25,** 4876–4882
31. Thompson, J. D., Higgins, D. G., and Gibson, T. J. (1994) *Nucleic Acids Res.* **22,** 4673–4680
32. Kelley, L. A., MacCallum, R. M., and Sternberg, M. J. (2000) *J. Mol. Biol.* **299,** 499–520
33. Rost, B. (1996) *Methods Enzymol.* **266,** 525–539
34. De Camilli, P., Vitadello, M., Canevini, M. P., Zanoni, R., Jahn, R., and Gorio, A. (1988) *J. Neurosci.* **8,** 1625–1631
35. Johnston, P. A., Cameron, P. L., Stukenbrok, H., Jahn, R., De Camilli, P., and Sudhof, T. C. (1989) *EMBO J.* **8,** 2863–2872
36. Erlander, M. G., and Tobin, A. J. (1991) *Neurochem. Res.* **16,** 215–226
37. Navone, F., Jahn, R., Di Gioia, G., Stukenbrok, H., Greengard, P., and De Camilli, P. (1986) *J. Cell Biol.* **103,** 2511–2527
38. Luzio, J. P., Brake, B., Banting, G., Howell, K. E., Braghetta, P., and Stanley, K. K. (1990) *Biochem. J.* **270,** 97–102
39. Reaves, B., Horn, M., and Banting, G. (1993) *Mol. Biol. Cell* **4,** 93–105
40. Letourneur, F., Gaynor, E. C., Hennecke, S., Demolliere, C., Duden, R., Emr, S. D., Riezman, H., and Cosson, P. (1994) *Cell* **79,** 1199–1207
41. Aridor, M., Bannykh, S. I., Rowe, T., and Balch, W. E. (1995) *J. Cell Biol.* **131,** 875–893
42. Orci, L., Stamnes, M., Ravazzola, M., Amherdt, M., Perrelet, A., Sollner, T. H., and Rothman, J. E. (1997) *Cell* **90,** 335–349
43. Nickel, W., Malsam, J., Gorgas, K., Ravazzola, M., Jenne, N., Helms, J. B., and Wieland, F. T. (1998) *J. Cell Sci.* **111,** 3081–3090
44. Nakamura, N., Rabouille, C., Watson, R., Nilsson, T., Hui, N., Slusarewicz, P., Kreis, T. E., and Warren, G. (1995) *J. Cell Biol.* **131,** 1715–1726
45. Orci, L., Ravazzola, M., and Perrelet, A. (1984) *Proc. Natl. Acad. Sci. U. S. A.* **81,** 6743–6746
46. Steiner, D. F., Docherty, K., and Carroll, R. (1984) *J. Cell. Biochem.* **24,** 121–130
47. Tooze, S. A., Hollinshead, M., and Dittie, A. S. (1994) *Biochimie* (*Paris*) **76,** 271–276
48. Cameron, P. L., Sudhof, T. C., Jahn, R., and De Camilli, P. (1991) *J. Cell Biol.* **115,** 151–164
49. Jean, C., Tollon, Y., Raynaud-Messina, B., and Wright, M. (1999) *Eur. J. Cell Biol.* **78,** 549–560
50. Jackson, C. L. (2000) in *Subcell. Biochem.* **34,** 233–272
51. Lippincott-Schwartz, J., Yuan, L., Tipper, C., Amherdt, M., Orci, L., and Klausner, R. D. (1991) *Cell* **67,** 601–616
52. Reaves, B., and Banting, G. (1992) *J. Cell Biol.* **116,** 85–94
53. Klausner, R. D., Donaldson, J. G., and Lippincott-Schwartz, J. (1992) *J. Cell Biol.* **116,** 1071–1080
54. Ladinsky, M. S., Mastronarde, D. N., McIntosh, J. R., Howell, K. E., and Staehelin, L. A. (1999) *J. Cell Biol.* **144,** 1135–1149
55. Donaldson, J. G., Lippincott-Schwartz, J., Bloom, G. S., Kreis, T. E., and Klausner, R. D. (1990) *J. Cell Biol.* **111,** 2295–2306
56. Seemann, J., Jokitalo, E., Pypaert, M., and Warren, G. (2000) *Nature* **407,** 1022–1026
57. Klumpermann, J., Kuliawat, R., Griffith, J. M., Geuze, H. J., and Arvan, P. (1998) *J. Cell Biol.* **141,** 359–371
58. Tsai, S.-C., Adamik, R., Hong, J.-X., Moss, J., Vaughan, M., Kanoh, H., and Exton, J. H. (1998) *J. Biol. Chem.* **273,** 20697–20701
59. Williger, B.-T., Provost, J. J., Ho, W. T., Milstine, J., and Exton, J. H. (1999) *FEBS Lett.* **454,** 85–89
60. Cherfils, J. (2001) *FEBS Lett.* **507,** 280–284
61. Worthylake, D. K., Rossman, K. L., and Sondek, J. (2000) *Nature* **408,** 682–688
62. Habets, G. G., Scholtes, E. H., Zuydgeest, D., van der Kammen, R. A., Stam, J. C., Berns, A., and Collard, J. G. (1994) *Cell* **77,** 537–549
63. Tarricone, C., Xiao, B., Justin, N., Walker, P. A., Rittinger, K., Gamblin, S. J., and Smerdon, S. J. (2001) *Nature* **411,** 215–219
64. De Camilli, P., and Jahn, R. (1990) *Annu. Rev. Physiol.* **52,** 625–645
65. Bock, J. B., Klumpermann, J., Davanger, S., and Scheller, R. H. (1997) *Mol. Biol. Cell* **8,** 1261–1271
66. Wong, S. H., Xu, Y., Zhang, T., Griffiths, G., Lowe, S. L., Subramaniam, V. N., Seow, K. T., and Hong, W. (1999) *Mol. Biol. Cell* **10,** 119–134
67. Kuliawat, R., Klumpermann, J., Ludwig, T., and Arvan, P. (1997) *J. Cell Biol.* **137,** 595–608
68. Dittie, A. S., Thomas, L., Thomas, G., and Tooze, S. A. (1997) *EMBO J.* **16,** 4859–4870
69. Arvan, P., and Castle, D. (1998) *Biochem. J.* **332,** 593–610
70. Tooze, S. A., Martens, G. J., and Huttner, W. B. (2001) *Trends Cell Biol.* **11,** 116–122
71. Stamnes, M. A., and Rothman, J. E. (1993) *Cell* **73,** 999–1005
72. Hirst, J., and Robinson, M. S. (1998) *Biochim. Biophys. Acta* **1404,** 173–193
73. Austin, C., Hinners, I., and Tooze, S. A. (2000) *J. Biol. Chem.* **275,** 21862–21869
74. D'Souza-Schorey, C., Boshans, R. L., McDonough, M., Stahl, P. D., and Van Aelst, L. (1997) *EMBO J.* **16,** 5445–5454
75. Solimena, M. (1998) *Diabetes Metab. Rev.* **14,** 227–240
76. Nozawa, K., Casiano, C. A., Hamel, J. C., Molinaro, C., Fritzler, M. J., and Chan, E. K. (2002) *Arthritis Res.* **4,** R3